ELSEVIER

Journal of Nuclear Materials 270 (1999) 357–367

journal of nuclear materials

Temperature dependence of the 20% cold worked 316 stainless steel steady state irradiation creep rate

John Paul Foster [a,*], Kermit Bunde [b], M.L. Grossbeck [c], E. Robert Gilbert [d]

[a] *Westinghouse Electric Company, Commercial Nuclear Fuel Division, 5801 Bluff Road, P.O. Drawer R, Columbia, SC 28250, USA*
[b] *Argonne National Laboratory, P.O. Box Idaho Falls, ID, USA*
[c] *Oak Ridge National Laboratory, Metals and Ceramics Division, P.O. Box Oak Ridge, TN, USA*
[d] *Pacific Northwest National Laboratory, Richland, WA, USA*

Received 24 June 1997; accepted 26 October 1998

Abstract

The irradiation creep data from four completed tests have been analysed to show that the steady state irradiation creep rate exhibits a moderate and complex temperature dependence. The irradiation creep tests were performed in the Experimental Breeder Reactor Number II (EBR-II) using beams and pressurized tubes, and in the Oak Ridge Reactor (ORR) and the High Flux Isotope Reactor (HFIR) using pressurized tubes. The data cover the temperature range from 200°C to 585°C, and show that from 200°C to 330°C, the steady state rate increases moderately with increasing temperature. At about 330°C, the steady state rate peaks and rapidly decreases with increasing temperature from 330°C to 370°C. From 370°C to 585°C the steady state rate moderately increases with increasing temperature.

1. Introduction

Irradiation creep has been studied extensively to provide data that can be used for component analysis. In the fast breeder program, irradiation creep has been investigated to characterize irradiation creep behavior and determine its interaction with swelling. This information is also useful for light water reactors where swelling is significantly reduced in comparison to fast breeders. In the case of Pressurized Water Reactors, the service behavior of baffle-former bolts and split pins in the reactor internals is dependent upon irradiation creep. Hence, the behavior of irradiation creep at relatively low dose levels needs to be characterized.

The irradiation creep strain of 20% cold worked (CW) 316 stainless steel (SS) [1] may be represented by an equation with three terms:

$$e = A_1\sigma[1 - \exp(-A_2 f)] + A_3\sigma f + A_4\Omega^2\sigma \ln(\cosh(f/\Omega)/A_5), \quad (1)$$

where e is the irradiation creep strain, σ is the stress, f is the displacement dose and A_1, A_2, A_3, A_4, A_5 and Ω are material coefficients. The first term is the initial transient component. The second term is the steady state rate component. The material coefficient A_2 provides a smooth transition between the transient and the steady state components. The third term is the tertiary component. The tertiary component has also been referred to as swelling enhanced irradiation creep and has been expressed in the form $D\Delta V/V_o$, where D is a material coefficient and $\Delta V/V_o$ is the swelling [2,3]. In this form, Eq. (1) becomes

$$e = A_1\sigma[1 - \exp(-A_2 f)] + A_3\sigma f + A_5\sigma(\Delta V/V_o). \quad (2)$$

Most emphasis has been placed on the swelling dependent component [4]. This study will re-evaluate the steady state rate term. Previous evaluations [1,3,5] have concluded that the steady state rate component is temperature independent. However, a detailed analysis of irradiation creep data over the temperature range of

* Corresponding author. E-mail: fosterjp@westinghouse.com

0022-3115/99/$ – see front matter
PII: S0022-3115(98)00748-X

200–585°C shows that the steady state component exhibits a complex temperature dependence. The purpose of this paper is to document this behavior. First, the selected irradiation creep tests will be analyzed and then the resulting temperature dependence of the steady state creep rate component will be presented.

2. Analysis of irradiation creep tests

The data from four completed irradiation creep tests will be analyzed to develop the temperature dependence of the steady state irradiation creep rate component. The tests covered a very wide temperature range. The tests include, pressurized tubes in Experimental Breeder Reactor Number II (EBR-II), beams in bending in EBR-II, pressurized tubes in Oak Ridge Reactor (ORR) and pressurized tubes in ORR/High Flux Isotope Reactor (HFIR).

A pressurized tube biaxial tension test [1,6] was performed in EBR-II. The test samples were short tubes fabricated with 20% CW 316 SS. The irradiation creep diametral strains were measured after fixed irradiation intervals. Fig. 1 presents a typical example of the data. The results show excellent self-consistency of the individual samples. The samples were tested in the temperature range of 377–585°C. Test data on different samples irradiated for different time periods provided irradiation creep data with increasing dose. The hoop strain versus hoop stress data were reported with neutron fluence units [1]. The displacement dose was calculated based on the sample axial locations at each measurement position and the neutron flux shape. The neutron flux values were calculated with the two-dimensional solver routines in the transport code DANTSYS. These evaluations used the ENDF/B-V cross sections and the sample radial–axial position geometry. The cross sections were collapsed to a 28 energy group structure using weighting fluxes appropriate for specific regions in the EBR-II core (the fuel, reflector and blanket regions). The 28 group damage cross sections were collapsed from ENDF/B-VI using the cross section processing code NJOY. The calculated displacement per atom values were determined by multiplying the neutron fluence by the ENDF/B-VI damage cross sections.

The irradiation creep coefficients were evaluated for each dose level using the hoop strain versus hoop stress data. A typical example is shown in Fig. 1. The irradiation creep coefficients were calculated by regression fits to the linear region of the hoop strain versus hoop stress at fixed dose levels. The hoop strain and stress units were converted to equivalent strain and stress using the reported conversion methods [7]. The EBR-II pressurized tube data and analysis was performed carefully to exclude the effects of swelling. In addition to the diameter measurements, length change and selected immersion density measurements were performed. These measurements were used to exclude the data sets that had swelling. In the absence of swelling, the resulting irradiation creep coefficients (i.e., in units of %/MPa-dpa)

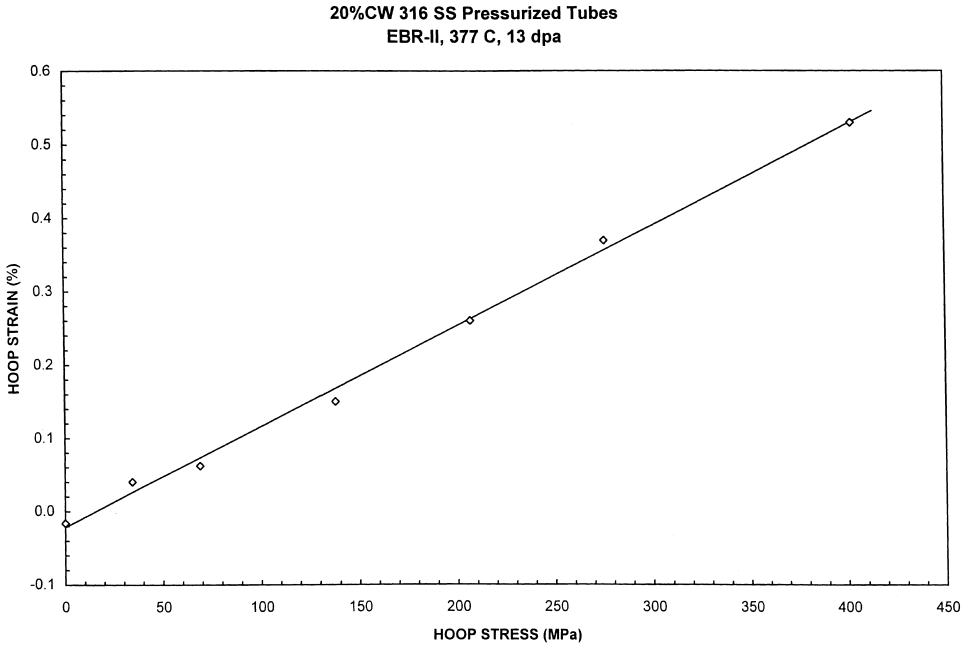

Fig. 1. Hoop strain versus hoop stress data for the EBR-II pressurized tube test at 377°C and 13 dpa.

should be approximately constant in the steady state rate region. Fig. 2 presents the data at a test temperature of 475°C. The irradiation creep coefficients are approximately constant over the dose range of 1.5–19.0 dpa as indicated by the solid line in Fig. 2. The irradiation creep coefficients at dose values greater than 19 dpa exhibit higher values due to tertiary or swelling enhanced creep as indicated by the dashed line in Fig. 2. The irradiation creep coefficients which exhibited approximately constant values at low dose levels were averaged as indicated in Fig. 2. This procedure was performed at each test temperature.

An irradiation creep in bending test [4,8–10] was performed in the EBR-II reactor. The beam samples were fabricated using 20% CW 316 SS. The beam samples included both 4-point uniform width and tapered width cantilever beams. The width of the cantilever beams were uniformly tapered such that a uniform bending stress resulted over the entire beam length. The data consist of repetitive strain measurements [4,8–10] made on the same samples with increasing dose. The displacement dose was calculated based on the beam axial locations at each measurement position and the neutron flux shape. The beam positions were determined from subassembly radiographs. The irradiation dose for each beam sample was calculated by the same procedure described above for the EBR-II pressurized tubes.

The beams were loaded with stresses over the range of 156–240 MPa for the cantilever and 80–327 MPa for the uniform beams, respectively. Since irradiation creep is linear with stress [1], the data were analysed as strain normalized stress versus dose. Figs. 3 and 4 present typical examples of the cantilever and 4-point beam data, respectively. The samples exhibit all three irradiation creep components (i.e., the initial transient, the steady state rate and the high dose tertiary component). The transient A_1 coefficient and the steady state rate coefficient A_3 were determined by regression fits to the data of the strain normalized stress versus dose in the linear region as illustrated in Figs. 3 and 4 for all of the beam samples. There were a total of 22 4-point and 42 cantilever beam samples. The beam bending creep coefficients used in this study were evaluated as carefully as possible to exclude the effects of swelling. According to Refs. [4,11], the creep behavior of the samples are linear up to about a fluence of 6×10^{22} n/cm^2 ($E > 0.1$ MeV). At fluences $>6 \times 10^{22}$ n/cm^2, the creep rate increases due to microstructural changes. These changes include swelling. A comparison of the maximum irradiation dose and irradiation temperatures of the beams evaluated in this study was made with the EBR-II pressurized tubes (for which immersion density data are available at relatively low doses). Further, the dose levels of the beam sample data set used in this study was significantly less than the dose level of the beam samples examined for swelling. Two uniform beams were destructively evaluated for swelling. The amount of swelling was small (<0.4%). The maximum dose values

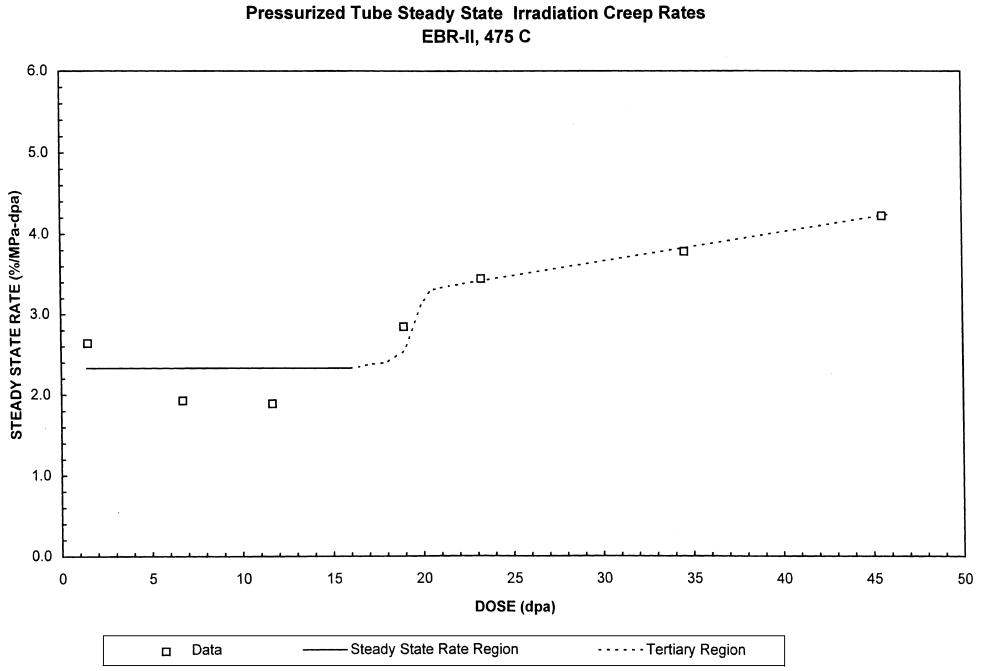

Fig. 2. Steady state creep rates from the EBR-II pressurized tube test at 475°C.

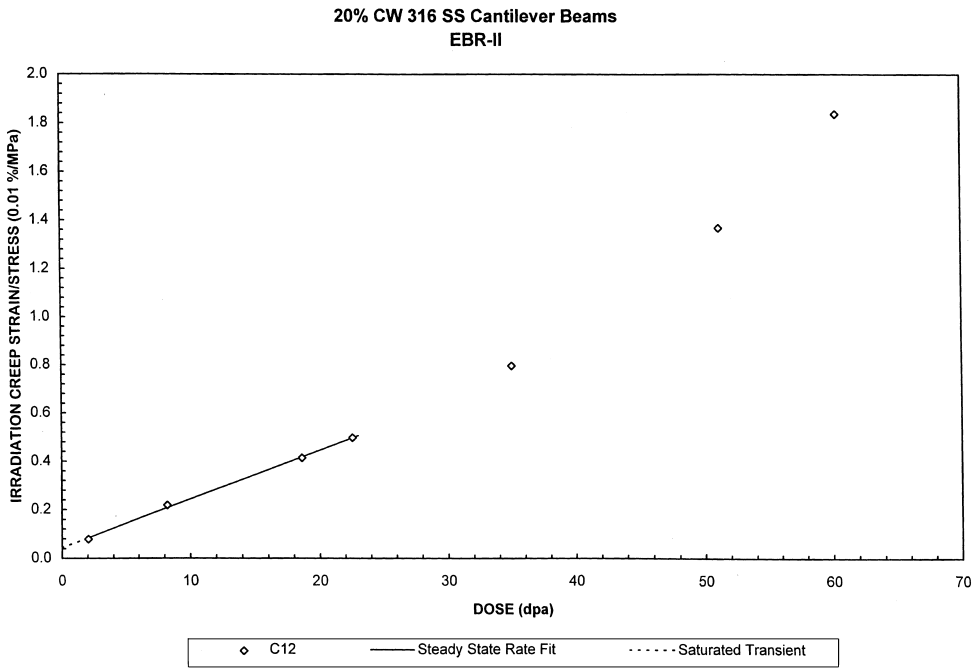

Fig. 3. Irradiation creep strain normalized stress versus dose data and the steady state rate regression fit for cantilever beam C12 in the EBR-II bending test.

of the data set used for the analysis presented by this study were significantly less than the dose values of the samples used for the swelling measurements.

Figs. 5 and 6 present the results for the transient A_1 and steady state rate A_3 coefficients, respectively. The cantilever beams with applied stresses below 156 MPa

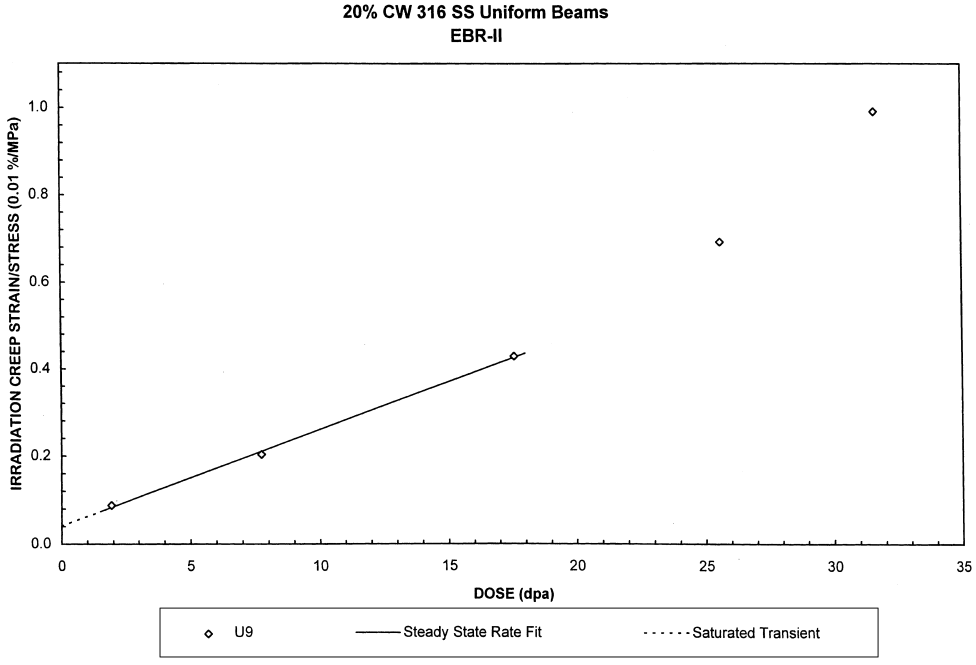

Fig. 4. Irradiation creep strain normalized stress versus dose data and the steady state rate regression fit for 4-point beam U1 in the EBR-II bending test.

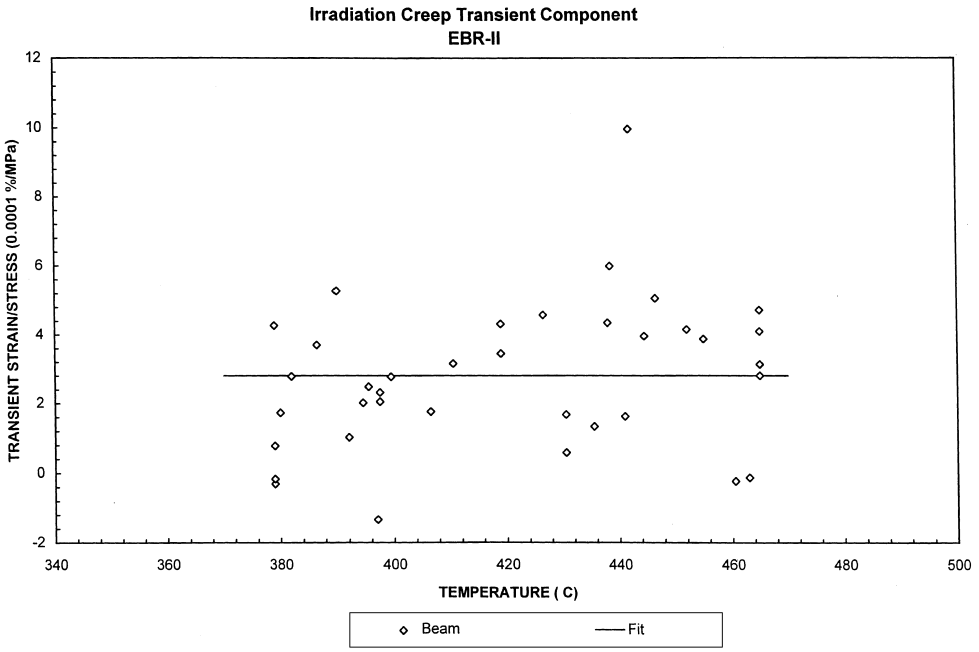

Fig. 5. Transient component A_1 coefficients for the cantilever and 4-point beams in the EBR-II bending test.

were neglected because very small irradiation creep strains were measured. The A_1 coefficient exhibits considerable scatter and is temperature independent over the range of 379–465°C. The steady state rate A_3 coefficient is temperature dependent. The value of A_3 decreases with decreasing temperature. The relatively moderate temperature dependence and beam sample-to-sample data scatter explain why the temperature dependence of the steady state rate was not previously observed. The steady state rate increase is only a factor

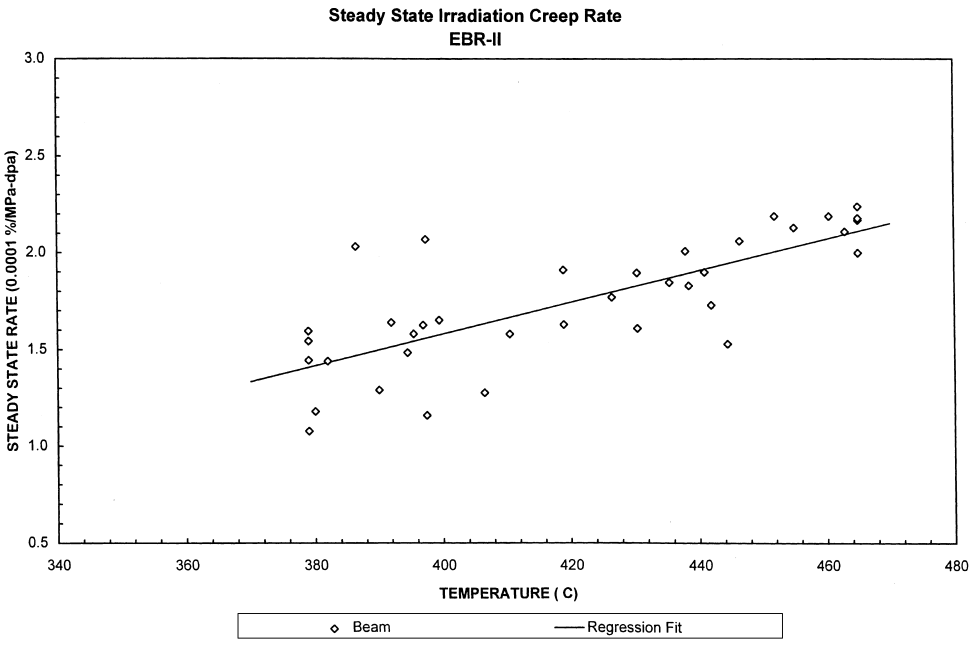

Fig. 6. Steady state rate component A_3 coefficients for the cantilever and 4-point beams in the EBR-II bending test.

of 1.5 from 379°C to 465°C. The line presented in Fig. 6 is a least square regression fit to the steady state rate data.

Two sets of pressurized tube tests [11,12] were performed in the ORR reactor. One set of 20% CW 316 SS samples were fabricated with heat number 15893. The samples were irradiated to 12 dpa over the temperature range of 330–600°C. Figs. 7 and 8 present the hoop strain and hoop stress data at 330°C and 400°C converted to equivalent strain versus equivalent stress. The higher temperature data at 500°C and 600°C were omitted because a careful reanalysis shows that it is inconsistent with the 330°C and 400°C data. All of the ORR data are presented in Figs. 7–10 as equivalent strain versus equivalent stress. Figs. 7 and 8 show that there is excellent sample-to-sample self consistency, and that the data extrapolate to small positive strain values (i.e., the y-intercept) at 0 stress. This extrapolation is considered to be representative of the stress free swelling. On the other hand, the data at 500°C and 600°C exhibit relatively large sample-to-sample scatter and an unreasonable y-intercept value in the case of the 500°C data. Fig. 9 shows that the 500°C data exhibit relatively large sample-to-sample scatter in comparison with the 330°C and 400°C data. Further, the y-intercept value is equal to -0.26%, which is inconsistent with the behavior exhibited by the 330°C, 400°C and 600°C data. In the case of the 600°C data (see Fig. 10), 5 data points are grouped at low stress and exhibit relatively large sample-to-sample scatter in comparison with the 330°C and 400°C data. Further, there is only one higher stress data point, so an accurate creep coefficient cannot be determined using this data set. Note that the y-intercept is apparently a small negative value between 0 and -0.1%.

The irradiation creep coefficients for the data in Figs. 7 and 8 were determined by regression fits to the linear region of the data. Since data at different dose levels are not available, the data in Figs. 7 and 8 were assumed to be in the steady state rate irradiation creep region. This is a reasonable assumption because the samples were irradiated to 12 dpa, which is considerably less than the dose levels required to initiate tertiary irradiation creep as illustrated by the EBR-II pressurized tube and beam tests (see Figs. 2–4).

A second set of pressurized tube samples [12] was fabricated with 20% CW 316 SS using a Japanese material heat. The samples were irradiated in ORR and then transferred to HFIR for continued testing. The samples were measured at 7 and 19 dpa. The steady state rate irradiation creep coefficients were determined by the method used for the first set of ORR pressurized tubes described above. Table 1 presents the results of a re-evaluation of the data used to formulate Table 3 in Ref. [11]. Note that the CW materials listed in Table 1 exhibit an increase in irradiation creep rate at 330°C relative to the results at 200°C and 400°C. The 25% CW USPCA results are listed as well as the 20% CW 316 SS results because the USPCA alloy is very similar in chemical composition to 316 SS. In addition, the thermo-mechanical treatment of both materials was similar. In the

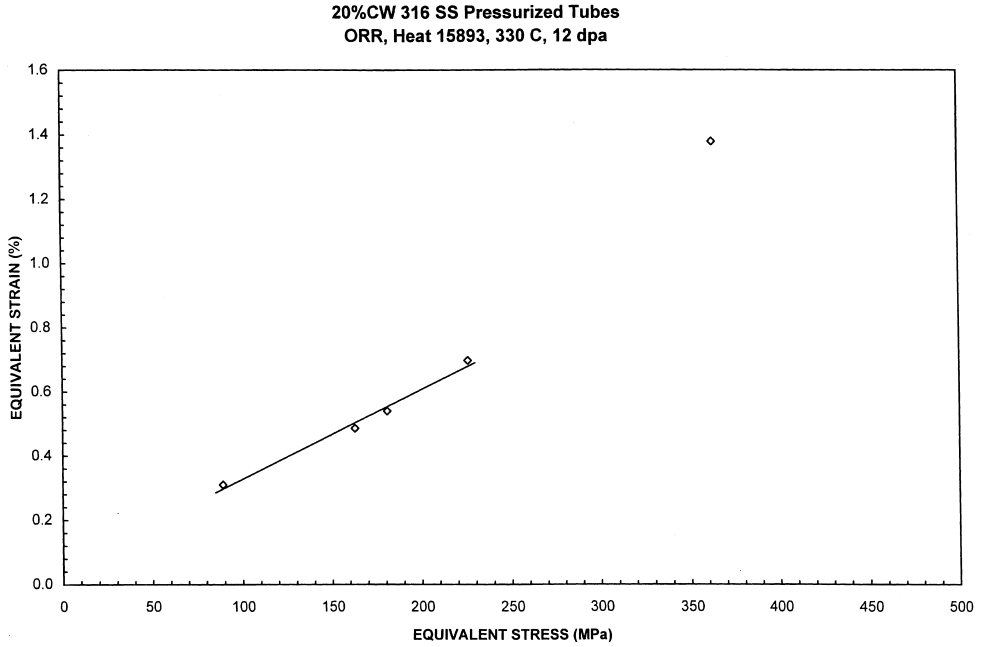

Fig. 7. Equivalent strain versus equivalent stress for the ORR Heat 15893 pressurized tubes at 330°C.

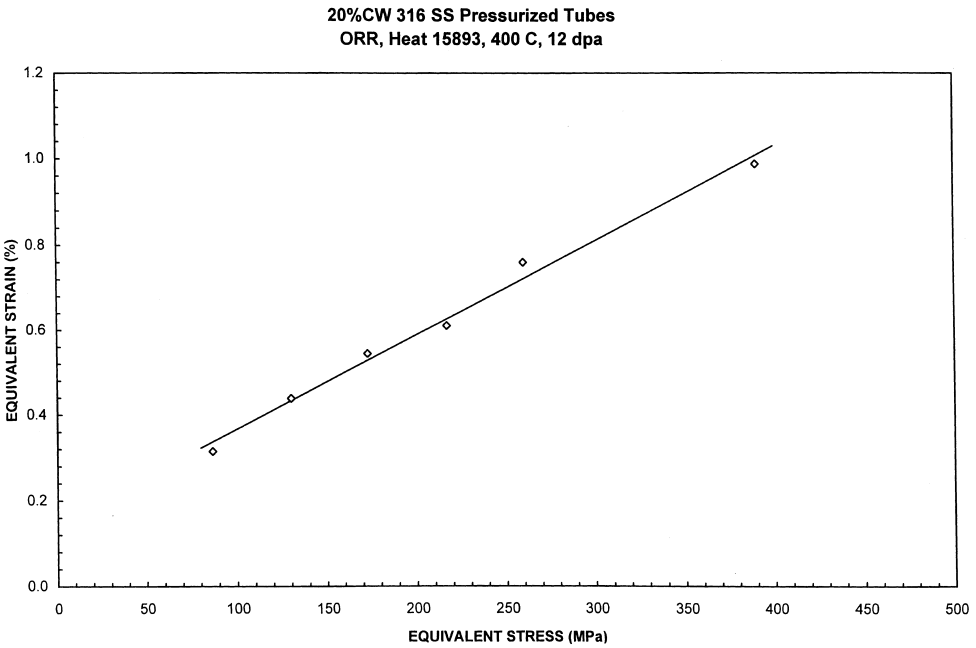

Fig. 8. Equivalent strain versus equivalent stress for the ORR Heat 15893 pressurized tubes at 400°C.

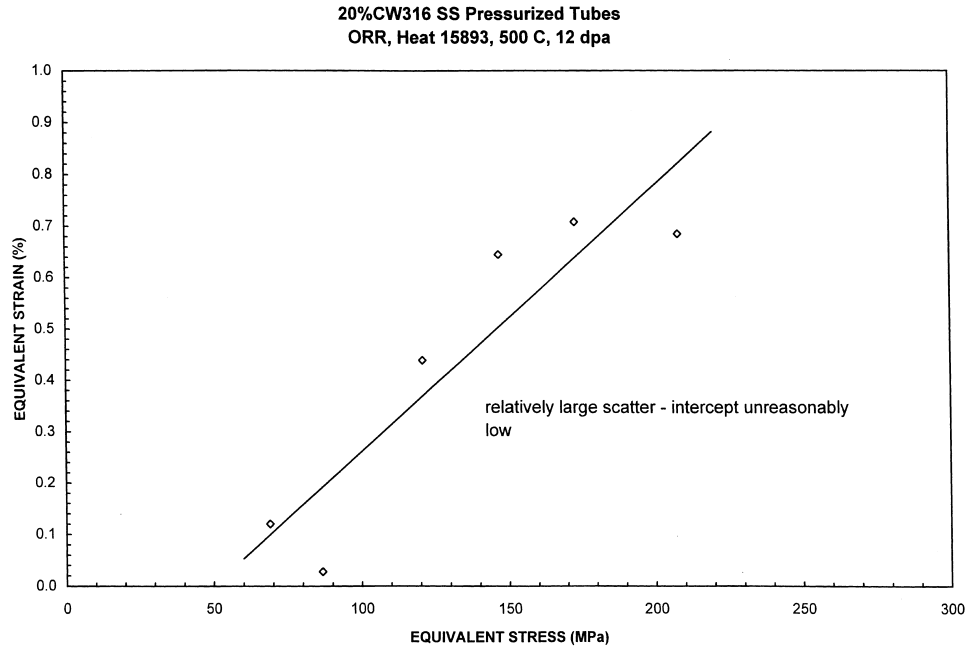

Fig. 9. Equivalent strain versus equivalent stress for the ORR Heat 15893 pressurized tubes at 500°C.

case of 20% CW 316 SS data at 7 dpa, the 330°C data show a small increase in the irradiation creep coefficient relative to the data at 200°C and 400°C. The USPCA suggest that this may be due to sample-to-sample data scatter. Confirmatory data for 20% CW 316 SS are required at 7 dpa.

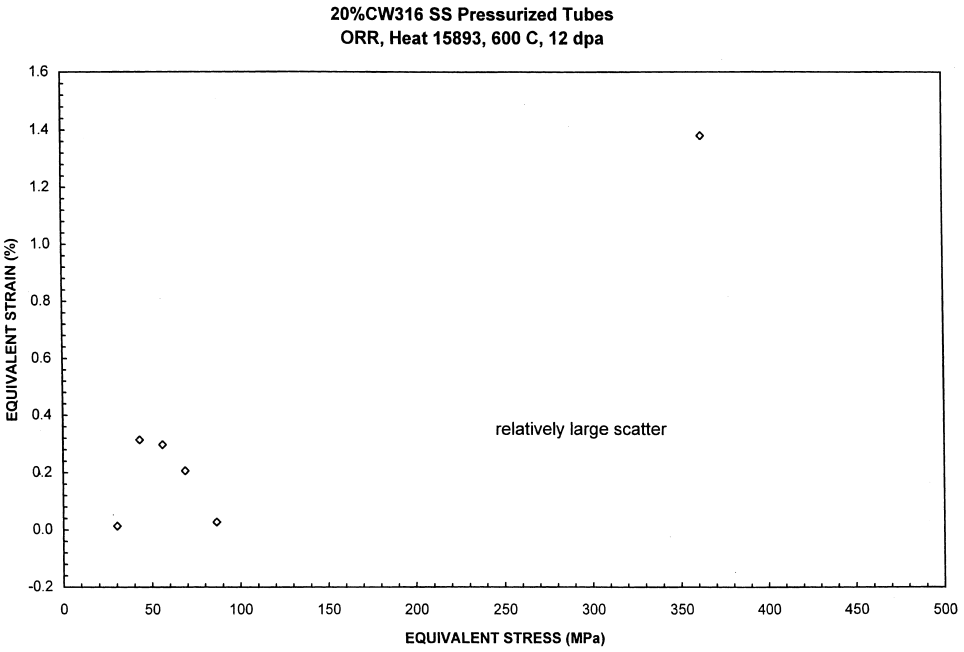

Fig. 10. Equivalent strain versus equivalent stress for the ORR Heat 15893 pressurized tubes at 600°C.

Table 1
Re-evaluated irradiation creep coefficients for 20% CW 316 SS and 25% CW USPCA alloys reported by Grossbeck and Horak [11]

Material	Dose (dpa)	Irradiation creep coefficient (10^{-6}/Mpa-dpa) at temperatures:			
		60°C	200°C	330°C	400°C
20% CW 316 SS	7	2.2	1.1	1.5	1.4
	19	–	0.70	2.2	1.1
25% CW USPCA	7	9.2–14	0.93	2.3	1.8
	19	–	0.63	2.7	1.5

3. Results and discussion

Fig. 11 presents the results of the steady state irradiation creep rate versus temperature. The data associated with each test is identified in the legend. The regression fit to the beams shown in Fig. 6 is presented in Fig. 11 and identified as the EBR-II beam test regression fit. The average steady state irradiation creep coefficients of the EBR-II pressurized tube test are identified as the EBR-II pressurized tubes. The irradiation creep coefficients determined at 12 dpa using the ORR biaxial stress test data are identified as ORR Heat 15893. The irradiation creep coefficients determined at 19 dpa using the Japanese 316 heat are identified as ORR Lot J316. The data in Fig. 11 cover an extensive temperature range from 200°C to 585°C. The ORR creep tests cover the range from 200°C to 400°C. As the temperature increases from 200°C to 370°C, the steady state rate moderately increases, peaks at about 330°C and then decreases at a rapid rate from 330°C to 370°C. Note that the irradiation creep coefficient results for the 25% CW USPCA alloy [12], which is similar in chemical composition to 316 SS, exhibit the same behavior in the temperature interval between 200°C and 400°C as illustrated in Fig. 11. The four data sets overlap in the temperature interval between 377°C and 400°C, and the steady state rates are in good agreement. The EBR-II pressurized tubes and EBR-II beams cover the range from 377°C to 585°C and exhibit a moderate increase in steady state creep rate with increasing temperature.

The comparison between EBR-II and ORR irradiation creep data may be made directly. Ref. [11] reported that higher irradiation creep occurs in ORR (a thermal neutron spectrum reactor) relative to FFTF (a fast neutron spectrum reactor). This apparent behavior was attributed to the higher amount of helium generated in the thermal neutron reactor. A re-examination of this analysis indicates that irradiation creep is similar in

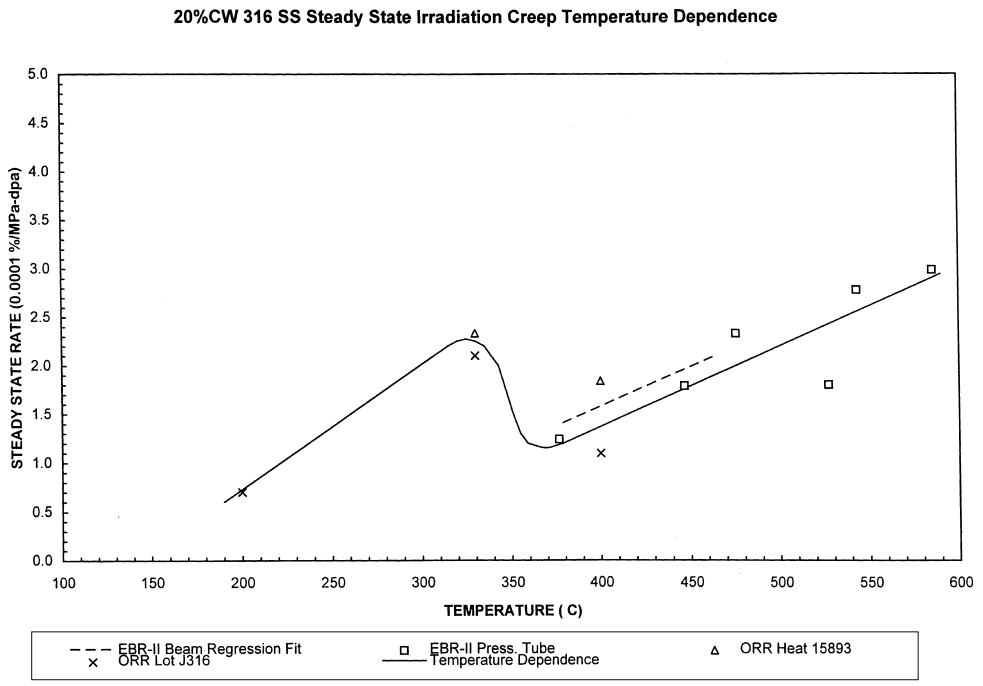

Fig. 11. Temperature dependence of the steady state irradiation creep rate.

thermal and fast neutron spectra. The comparison of the ORR and FFTF data can only be performed by using a dose extrapolation. Figs. 3–5 presented by Grossbeck and Horak [11] show that the ORR and FFTF data do not overlap in dose. The FFTF data must be extrapolated to lower dose values in order to be compared with

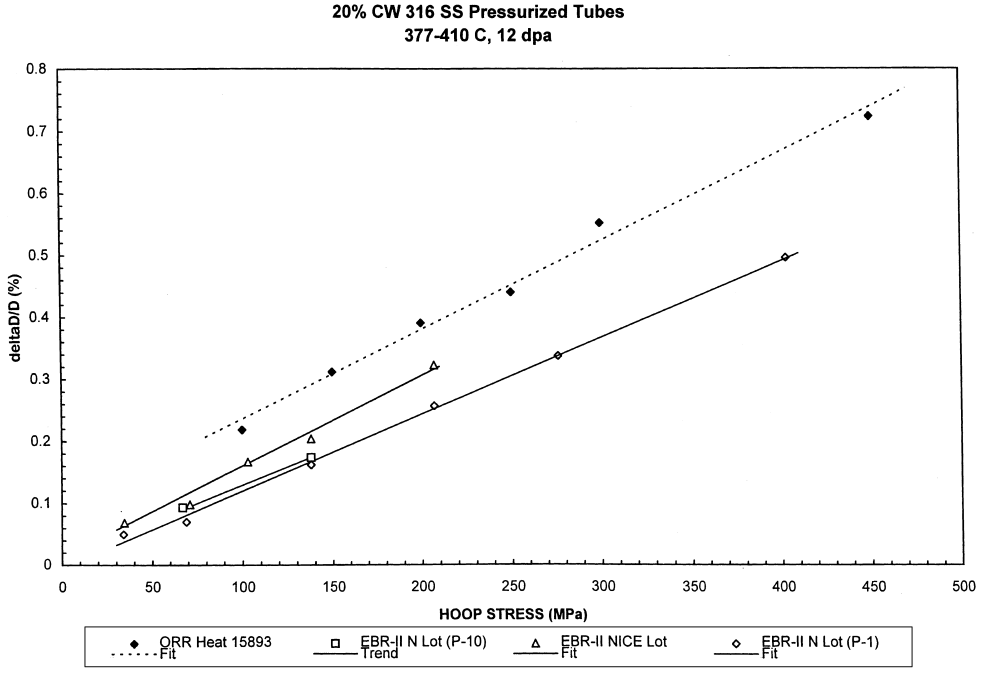

Fig. 12. Hoop strain versus hoop stress of pressurized tubes irradiated in ORR and EBR-II in the temperature range from 377°C to 410°C at 12 dpa.

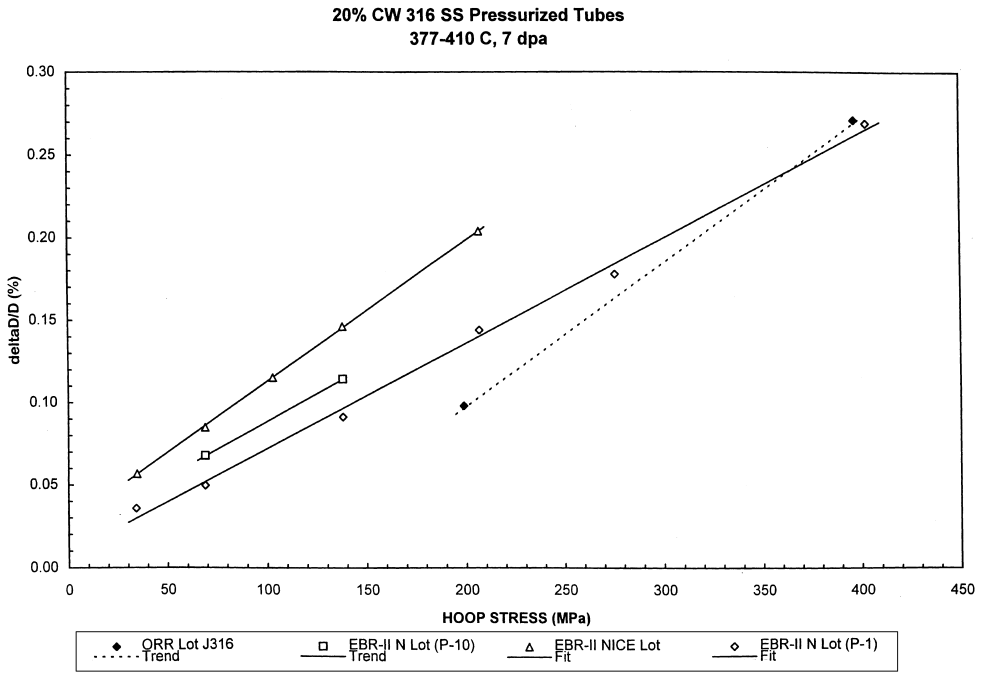

Fig. 13. Hoop strain versus hoop stress of pressurized tubes irradiated in ORR and EBR-II in the temperature range from 377°C to 410°C at 7 dpa.

the ORR data. However, if the EBR-II data are used for the comparison with the ORR data rather than the FFTF data, no extrapolation in dose is required. Figs. 12 and 13 present the ORR and EBR-II data. Fig. 12 shows at 12 dpa that the irradiation creep strain in ORR is slightly higher than in EBR-II. On the other hand, Fig. 13 shows at 7 dpa that the ORR samples exhibit slightly less irradiation creep strain than the EBR-II samples. Hence, when the thermal spectra (ORR) and the fast spectra (EBR-II) samples are compared over the same dose interval (and at the same irradiation temperature) no significant difference in irradiation creep strain is apparent. The slight shift of the ORR data from slightly less to slightly higher irradiation creep relative to the EBR-II data at 7 and 12 dpa may be due to helium generation as a function of increasing dose. Alternatively, this slight shift could be simply due to sample-to-sample scatter. These results show that helium does not have a large effect on irradiation creep at relatively low dose levels. Hence, the EBR-II and ORR data may be directly compared as presented in Fig. 11.

4. Conclusions

A detailed analysis of irradiation creep test data show that the steady state irradiation creep rate exhibits a moderate and complex temperature dependence in the temperature range from 200°C to 585°C. From 200°C to 330°C, the steady state rate increases moderately with increasing temperature. At 330°C the steady state rate peaks, and rapidly decreases from 330°C to 370°C. From 377°C to 585°C, the steady state rate moderately increases with increasing temperature.

Acknowledgements

The authors are grateful to Mr James Rex and Mr David Boyle (Westinghouse/Nuclear Service Division) for programmatic support, to Dr Douglas Porter (Argonne National Laboratory/West) for coordinating the dose calculations and technical discussions. This work was supported by the Southern Nuclear Operating Company, the Westinghouse Owner's Group and Westinghouse Electric Corporation.

References

[1] R.J. Puigh, E.R. Gilbert, B.A. Chin, in: Effects of Radiation on Materials, H.R. Brager, J.S. Perrin (Eds.), Eleventh Conference, ASTM STP 782, American Society for Testing and Materials, 1982.
[2] R.A. Weiner, J.P. Foster, A. Boltax, in: Radiation Effects in Breeder Structural Materials, AIME June (1977) 865.

[3] D.L. Porter, E.L. Wood, F.A. Garner, in: Effects of Radiation on Materials, 14th International Symposium, vol. II, ASTM STP 1046, 1990, p. 551.
[4] J.M. Rosa, T. Lauritzen, W.L. Bell, G.M. Konze, S. Vaidyanathan, C1 Irradiation Creep in Bending Experiment, Evaluation and PIE Results, General Electric Company Report GEFR-00637, September 1982.
[5] F.A. Garner, in: Proceedings of the 10th International Symposium on Environmental Degradation of Materials in Nuclear Power Systems – Water Reactors, Amelia Island, August 1997.
[6] E.R. Gilbert, J.F. Bates, J. Nucl. Mater. 65 (1977) 204.
[7] E.R. Gilbert, L.D. Blackburn, J. Eng. Mater. Tech. 99 (1977) 168.
[8] J. Marshall, A.J. McSherry, M.R. Patel, P.J. Ring, W.K. Appleby, J. Nucl. Mater. 66 (1977) 230.
[9] J.M. Rosa, Irradiation Creep in Bending of 20% CW 316: C1 Results at 12×10^{22} n/cm^2, General Electric Company Report GEFT-00577, September 1981.
[10] T. Lauritzen et al., Effects of Radiation on Materials, ASTM STP 955.
[11] M.L. Grossbeck, J.A. Horak, J. Nucl. Mater. 155–157 (1988) 1001.
[12] M.L. Grossbeck, L.T. Gibson, S. Jitsukawa, L.K. Mansur, L.J. Turner, Effects of radiation on materials, in: 18th International Symposium, ASTM STP 1325, 1977.